Layered Gradient Nonwovens of In Situ Crosslinked Electrospun Collagenous Nanofibers Used as Modular Scaffold Systems for Soft Tissue Regeneration

*Marco Angarano, Simon Schulz, Martin Fabritius, Robert Vogt, Thorsten Steinberg, Pascal Tomakidi, Christian Friedrich, and Rolf Mülhaupt**

In a versatile modular scaffold system, gradient nonwovens of in situ crosslinked gelatin nanofibers (CGN), fabricated by reactive electrospinning, are laminated with perforated layers and nonwovens of thermoplastic non-crosslinked biodegradable polyesters. The addition of glyoxal to a gelatin solution in a non-toxic solvent mixture consisting of acetic acid, ethyl acetate, and water (5:3:2 w/w/w) enables the in situ crosslinking of gelatin nanofibers during electrospinning. The use of this fluorine-free crosslinking system eliminates the need of post-treatment crosslinking and purification steps typical for conventional CGN scaffolds. The slowly progressing crosslinking of the dissolved gelatin in the presence of glyoxal increases the viscosity of the gelatin solution during electrospinning so that the average diameter of the crosslinked gelatin nanofibers gradually increases from 90 to 680 nm. During the subsequent lamination process, alternating layers of CGN and polycaprolactone (PCL) nonwovens, produced by 3D microextrusion of micrometer-sized PCL fibers, are bonded together upon heating above the PCL melting temperature. In contrast to the water-soluble gelatin nanofibers and the comparatively weak CGN, the CGN/PCL/CGN layered biocomposites are water-resistant and very robust. In such modular scaffold systems, strength, biodegradation rate, and biological functions can be controlled by varying the type, composition, fiber diameter, porosity, number, and sequence of the individual layers. The CGN/PCL multilayer biocomposites can be cut into any desired scaffold shape and attached to tissue by surgical sutures in order to suit the needs of individual patients.

1. Introduction

Regenerative medicine represents a rapidly progressing field with interdisciplinary interplay at the frontiers of materials science, bioengineering, cell biology, and biomedicine.[1] One of the main challenges for material scientists in tissue engineering is the development of scaffolds as three-dimensional templates that mimic the extracellular matrix (ECM) and enable tissue regeneration. Resembling fibrous ECM structures with their nanometer-scaled dimensions, nanofiber nonwovens as well as micro-/nanohybrid nonwovens are well recognized as very promising candidates for scaffold fabrication owing to their extremely large specific surface area combined with facile tailoring of binding sites on the nanofiber surfaces.[2–4] Compared to conventional macro- and microporous scaffolds, collagenous nanofiber nonwovens require much smaller cell concentrations to enable effective cell seeding, cell adhesion and proliferation. Moreover, cell growth and effective diffusion of nutrients and oxygen are not restricted to the scaffold surface but take place throughout the entire scaffold. Among polymer processing technologies, electrospinning represents the leading technology with high cost-effectiveness and extraordinary versatility in terms of tailoring multifunctional nanofiber and nonwoven architectures. In the high-voltage electrical field between the injector and the collector, the jet stream of a polymer solution emerges from a capillary tube of a syringe and deposits a random pattern of dry ultrafine fibers on the collector, thus producing nanofiber nonwovens. A remarkably wide variety of polymers has been converted into nanometer- and micrometer-sized fiber nonwovens by means of electrospinning.[1,5,6] In recent years, electrospinning has been successfully applied to fabricate biomimetic protein nanofiber scaffolds.[7] Electrospinning of synthetic and natural polymers has been used to design ECM-like nonwovens as model systems to achieve a better understanding of biocompatibility and cell proliferation characteristics. For example, synthetic biodegradable polymers such as polycaprolactone (PCL)[8–11] and polylactide (PLA)[12–14] were successfully electrospun and tested in vitro. In spite of their excellent mechanical strength, most synthetic polymers were found to be inferior to natural biopolymers, which afford much better cell adhesion combined with more effective cell proliferation. As a

M. Angarano, M. Fabritius, Prof. C. Friedrich, R. Vogt, Prof. R. Mülhaupt
Freiburg Materials Research Center (FMF) and Institute for Macromolecular Chemistry of the Albert-Ludwigs University Freiburg
Stefan-Meier-Str. 31, D-79104 Freiburg, Germany
E-mail: rolf.muelhaupt@makro.uni-freiburg.de
Dr. S. Schulz, Prof. T. Steinberg, Prof. P. Tomakidi
Department of Oral Biotechnology, Dental School University Hospital Freiburg
Hugstetterstrasse 55, D-79106 Freiburg, Germany

DOI: 10.1002/adfm.201202816

consequence, natural biopolymers, such as gelatin, were blended with synthetic polymers such as PCL,[15,16] PLGA, and PLA,[17] for applications in electrospinning.[18] In another approach toward improving the performance of synthetic polymers, gelatin was grafted onto synthetic fibers.[19,20] Compared to their fully synthetic counterparts, both blends and grafts afforded markedly improved cell growth. Furthermore, the incorporation of natural biopolymer nanofibers provided far superior biocompatibility and excellent cell adhesion owing to the presence of effective binding sites that guide cell adhesion, ECM formation, and cell proliferation.[21] However, both their high degree of water swelling and their inherent lack of mechanical stability in an aqueous medium represent striking drawbacks typical of most natural polymers, particularly water-soluble gelatin. This is very problematic with respect to their envisioned applications in surgery. Therefore, extensive research has been aimed at post-spinning crosslinking, thus rendering nanofibers water-resistant without sacrificing cell adhesion and bioresorption.[21–25] Typically, post-spinning crosslinking of collagenous nanofibers involves gas-phase crosslinking using glutaric aldehyde vapor,[23–25] genipin[22,25] or D,L-glyceraldehyde[25] as crosslinking agents. However, most of these two- or multistep processes are tedious, expensive, and difficult to implement into scaled-up fabrication of nonwovens. In view of scaffold manufacturing and the envisioned applications, it is highly desirable to eliminate post-treatment steps by enabling in situ crosslinking during electrospinning. A one-step electrospinning process for the in situ crosslinking of chitosan nanofibers, which produces water-, base-, and acid-resistant chitosan nonwovens, was developed by Schiffman and Schauer, who added glutaric aldehyde as a crosslinking agent to chitosan solutions in trifluoroacetic acid prior to electrospinning.[23] They demonstrated that their one-step process was 25 times faster than the two-step process using post-electrospinning crosslinking. Nguyen et al. described the first successful in situ crosslinking of gelatin during electrospinning. They used a very small amount of glutaric aldehyde as a crosslinking agent for gelatin solutions in trifluoroacetic acid.[26] In addition to strong acids, other preferred fluorine-containing solvents for dissolving gelatin include highly toxic fluorinated alcohols such as 1,1,1,3,3,3-hexafluoro-2-propanol and 2,2,2-trifluoroethanol (TFE). With regard to scale-up and commercial applications, the elimination of fluorine-containing, toxic, and highly corrosive solvents has very high priority with respect to eliminating potential pollution and health hazard problems. Furthermore, meeting the stringent demands of medical applications would require extensive purification to ensure the quantitative removal of trace amounts of residual toxic fluorinated compounds. Owing to the formation of very strong hydrogen bridges between proteins and fluorinated acids and alcohols, this purification is rather difficult for protein fibers. In their co-solvent approach, Song et al. developed a fluorine-free solvent system for electrospinning non-crosslinked gelatin nanofibers using a mixture of acetic acid, ethyl acetate, and water (5:3:1 w/w/w).[27] Recently Wnek et al. developed a in situ crosslinking method for electrospun gelatin fibers. They used 1-ethyl-3-(3-dimethyl-aminopropyl)-1-carbodiimide hydrochloride (EDC) and N-hydroxysuccinimide (NHS) as crosslinker-system in collagen-ethanol-PBS solution. After storing the fibers at a controlled humidity of 43% for three days they obtained water-stable fiber-mats.[28] In spite of this successful fabrication of gelatin nanofiber nonwovens by means of electrospinning, most state-of-the-art gelatin-based nonwovens lack mechanical stability in an aqueous environment. This prerequisite is critical for the successful application of scaffolds in surgery because this requires manipulation of the scaffolds in an aqueous medium, their subsequent transfer from cell cultures without loss of structural integrity, and to their attachment healthy tissue by means of surgical sutures. In recent approaches towards manufacturing of scaffolds, the use of solid freeform fabrication in rapid prototyping exploits computer-guided layer-by-layer manufacturing to produce scaffolds with tailored pore size, pore distribution, and porosity.[29–34] For example, solid freeform fabrication was employed to fabricate a variety of collagen scaffolds with internal vascular architectures.[35] Whereas most rapid prototyping processes are restricted to highly specialized formulations, the 3D microextrusion process (also known as 3D dispensing, 3D microplotting, 3D Bioplotting, or 3D fiber deposition) is extraordinarily versatile with respect to the very wide choice of materials, which ranges from ceramic and metal pastes to polymer melts, dispersions, solutions, and even hydrogel precursors.[36] According to CAD/CAM-3D dispensing results, the patterns of the 3D-deposited micrometer-sized strands are readily varied, producing scaffolds with controlled 3D architectures and interconnected micrometer-sized pores.[34–37] Compared to the electrospun nonwovens with large specific surface areas, the 3D-plotted structures afford much larger fiber diameters, larger pores, and fewer binding sites on the surface, thus accounting for lower cell seeding effectiveness and higher mechanical stability in an aqueous medium. It is thus desirable to combine the structural features typical of electrospinning and 3D fiber deposition. The resulting scaffolds with hierarchical architectures contain ECM-like electrospun layers with large specific surface areas. These function as "cell sieves" with effective binding and ECM-like stimulation of cell proliferation, whereas the layers of macroporous nonwovens provide reinforcement and robustness. This intriguing concept of hierarchical electrospun multilayer scaffolds was first achieved by the groups of van Blitterswijk[41] and Kim[42,43] by integrating electrospinning into the 3D fiber microextrusion process. Electrospinning of fibers (10 μm) on 3D-plotted fiber webs (300 μm) was reported to enhance cell entrapment and the wetting capabilities of such scaffolds.[41] Moreover, it was observed that chondrocytes maintained their rounded morphology in hierarchical scaffolds, whereas they spread in conventional scaffolds produced by 3D microextrusion.[41] Electrospinning of PCL/small intestine submucosa and PCL/silk fibroin blends directly onto 3D-plotted microstrands afforded hierarchical biocomposites exhibiting both markedly improved cell adhesion and proliferation of bone marrow-derived mesenchymal stem cells.[42]

Herein we report on the development of modular scaffold systems and micro-/nanohybrid biocomposites in which collagenous nanofiber nonwovens, produced by electrospinning and in situ crosslinking, are laminated with bioresorbable polyester layers that serve simultaneously as a perforated hotmelt adhesive patch and as reinforcement. An important objective has been the in situ crosslinking of gelatin nanofibers during electrospinning by the use of nontoxic, fluorine-free crosslinking systems, thus aiming at the fabrication of gradient nonwovens with average

Table 1. The in situ crosslinked samples.

Sample	Gelatin concentration [wt%]	Solvent	Crosslinker	n(Crosslinker)/m(Gelatin) [mol·g^{-1}]
gel14/42	14	AWE[a)]	glyoxal	42×10^{-5}
gel14/74	14	AWE[a)]	glyoxal	74×10^{-5}
gel14/158	14	AWE[a)]	glyoxal	158×10^{-5}
gel14/195	14	AWE[a)]	glyoxal	195×10^{-5}
gel14/GTA13	14	AWE[a)]	GTA[c)]	13×10^{-5}
gel8TFE/135	8	TFE[b)]	glyoxal	135×10^{-5}

[a)]Acetic acid/ethyl acetate/water (5:3:2 w/w/w): [b)]TFE: trifluoroethanol; [c)]glutaric aldehyde.

fiber diameters that gradually increase from 100 to 1000 nanometer during electrospinning. This lamination process is very versatile and does not require integration of the electrospinning process into the fabrication of porous polyester layers. The influences of glyoxal content, solvents, processing conditions and gradient formation on nonwoven architectures, cell adhesion properties, water-resistance, water-swelling, and the mechanical properties in an aqueous medium are investigated.

2. Results

In the modular system, electrospun in situ crosslinked gelatin nonwovens (CGN) with nanometer-sized fiber diameters were bonded together with non-crosslinked 3D-microextruded PCL nonwovens with micrometer-sized fiber diameter by heating the multilayer system above the PCL melting temperature. To reduce water-swelling and improve water resistance it is imperative to crosslink gelatin nanofibers during electrospinning without using toxic fluorinated solvents. In our "mixing prior to spinning" process, glyoxal and glutaric aldehyde (GTA) were added as crosslinking agents to gelatin dissolved in a solvent mixture consisting of acetic acid, water, and ethyl acetate (5:2:3 w/w/w), denoted hereinafter as AWE. For comparison, trifluoroethanol (TFE) was also used as solvent. As shown in **Table 1**, the gelatin content, the amount of crosslinking agent, and the process conditions were varied systematically to optimize the conditions for in situ crosslinking of gelatin. An important objective was to match the crosslinking rate and the duration of electrospinning. Slow crosslinking speed is essential to assure the pot life of the gelatin solution containing the crosslinking reagent in order to enable stable electrospinning for several hours without premature gelation of the gelatin solution in the feed system. The influence of these parameters on the nonwoven architectures was determined by means of scanning electron microscopy (SEM). After immersing the laminated CGN/PCL micro-/nanohybrid scaffolds in water, stress/strain testing was employed to measure the mechanical properties of the nonwovens in an aqueous environment.

2.1. Monitoring in situ Crosslinking

The viscosity of the spinning dope is one of the key parameters governing electrospinning. The average diameter of electrospun fibers generally increases with increasing solution viscosity until a high viscosity and degree of gelation render electrospinning impossible. The viscosity is a function of the gelatin content and the polymer molecular weight. When crosslinking agents such as glyoxal and glutaric aldehyde (GTA) are added to the gelatin solution, chain extension accounts for molecular weight build-up and increased viscosity. As soon as many gelatin molecules are linked together, networks are formed, accompanied by a drastic increase in viscosity and gelation. Owing to the comparatively low throughput of this electrospinning process in which spinning takes several hours, the crosslinking rate must be adjusted to the spinning time, thus preventing processing problems relating to premature gelation accompanied by plugging of the feed lines. The influence of the glyoxal content was monitored by means of solution rheology by measuring changes of the solution viscosity (η), the storage modulus (G'), and the loss modulus (G'') as a function of time. For comparison and as a benchmark to the state-of-the-art solvent systems, gelatin was crosslinked with glyoxal in trifluoroethanol (gel8TFE/135, Table 1) and with GTA in the AWE solvent mixtures (gel14/GTA13, Table 1). As is apparent from **Figure 1**, crosslinking gelatin solutions with glyoxal in AWE is a relatively slow process; however, it can be readily controlled by varying the glyoxal/gelatin ratio and matching the required pot life of the gelatin solutions for electrospinning. Doubling the glyoxal content decreased the gel time (measured as G' *equal*

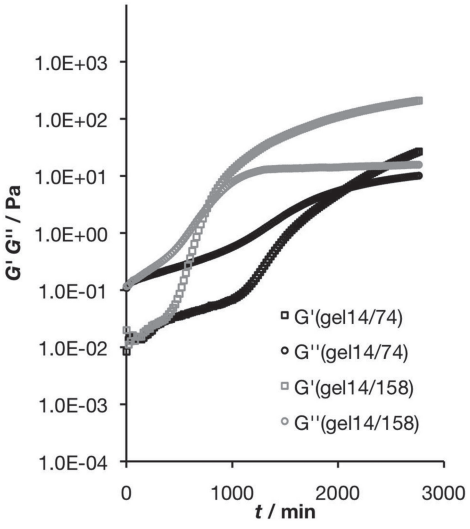

Figure 1. Storage (G') and loss modulus (G'') as a function of time for gelatin/AWE using two different glyoxal contents: 74×10^{-5} mol·g^{-1} (gel14/74) and 158×10^{-5} mol·g^{-1} (gel14/158).

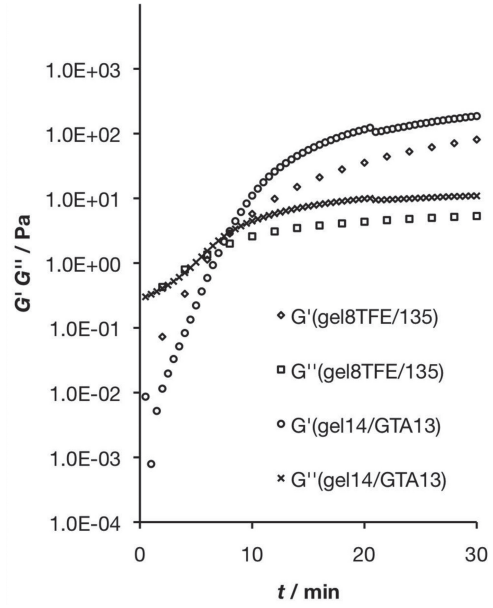

Figure 2. Storage (*G′*) and loss modulus (*G″*) for glyoxal-mediated crosslinking in TFE (gel8TFE/135) and for gelatin crosslinking in AWE using GTA as the crosslinking agent (gel14/GTA13).

to G″) from 2100 to 600 min. In sharp contrast, as shown in **Figure 2**, replacing glyoxal by GTA and substituting the fluorine-free AWE solvent mixture by fluorine-containing TFE led to drastically increased crosslinking rates with much shorter gel times of only a few minutes after mixing the components. This striking difference in reactivity is also clearly visible in **Figure 3**, which shows the solution viscosity as a function of time for various solvents and crosslinking systems. Whereas all gelatin/glyoxal mixtures in the AWE solvent mixtures afforded a relatively slow viscosity increase over a period of many hours, an instantaneous viscosity build-up was observed for both TFE solvents and GTA addition. On the basis of the gel times and the above rheological measurements, TFE- and GTA-mediated rapid crosslinking reactions do not meet the requirements of the electrospinning process. Therefore, it is not surprising that all our attempts to use GTA-mediated crosslinking in electrospinning of gelatin have failed. In fact, we observed instant gelation when a droplet of GTA was added to a TFE solution of gelatin. In contrast to TFE and GTA, the use of glyoxal together with the fluorine-free AWE solvent system offers a much broader processing window, thus enabling in situ crosslinking of gelatin solutions during electrospinning and easy process control.

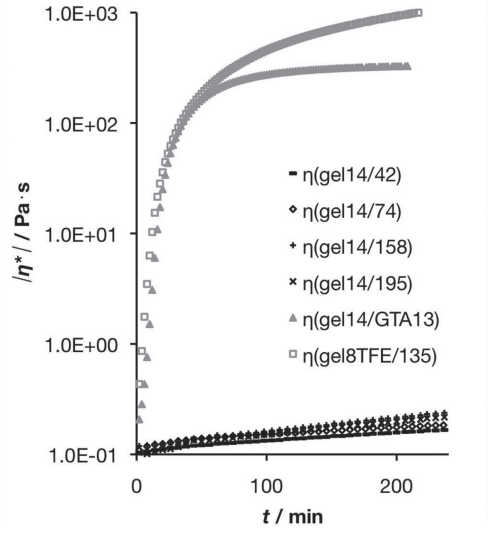

Figure 3. The solution viscosity as a function of time for various types and amounts of crosslinking agents and fluorinated and fluorine-free solvents.

2.2. Morphologies of CGN Nonwovens

As illustrated in **Figure 4**, electrospun samples of the nonwovens, which were prepared by in situ by glyoxal-mediated crosslinking of gelatin dissolved in AWE (gel14/158, Table 1), were recovered during electrospinning and investigated by means of scanning electron microscopy (SEM). **Table 2** lists the observed average fiber diameters with respect to time. Obviously, the increase in solution viscosity during electrospinning was paralleled by an increase in CGN diameters, as reflected by the formation of a distinct fiber diameter gradient. Small fiber diameters of around 90 nm were formed in the bottom layer of the CGN nonwovens. As the viscosity increased during electrospinning, the fiber diameter gradually increased, approaching 680 nm in the top layer after electrospinning for 240 min. Hence, matching of crosslinking and electrospinning rates provides a means to control gradient formation during electrospinning.

Water resistance and crosslinking: To assess crosslinking resulting from glyoxal addition, we examined water-uptake and monitored conversion of the primary amino groups as a function of the glyoxal content. Whereas non-crosslinked gelatin nanofibers disintegrate and dissolve immediately upon contact with water, the addition of small amounts of glyoxal to the gelatin solutions renders CGN nonwovens water-resistant without eliminating high water-uptake. In fact, the CGN nonwovens can be stored in water for a prolonged period of time without loosing their structural integrity. **Table 3** lists the water uptake, as measured after immersing the CGN nonwovens in distilled water for 24 h at 37 °C. The samples were pressed between filter papers until the filter papers stopped showing any signs of wetting. Although it is not possible to distinguish between water uptake resulting from adsorption and nanofiber swelling, all CGN nonwovens exhibited around 260% water uptake with respect to their weight prior to immersion in water. At the lowest glyoxal content, which is equivalent to the lowest crosslink density, the water uptake increased to 370% without adversely affecting the structural integrity of the CGN nonwovens. For the envisioned applications in tissue engineering, this high water uptake is quite beneficial and reflects a high hydrophilicity as well as excellent wetting of CGN nonwovens.

The crosslinking reaction was monitored by determining the conversion of primary amine groups as a function of the glyoxal/gelatin ratio using a 2,4,6-trinitrobenzenesulfonic acid (TNBS) assay according to procedures described by Bubnis and Ofner.[44,45] It should be noted that this amine conversion is only a qualitative measure of the crosslinking density because glyoxal can react with a primary amine group without necessarily contributing to

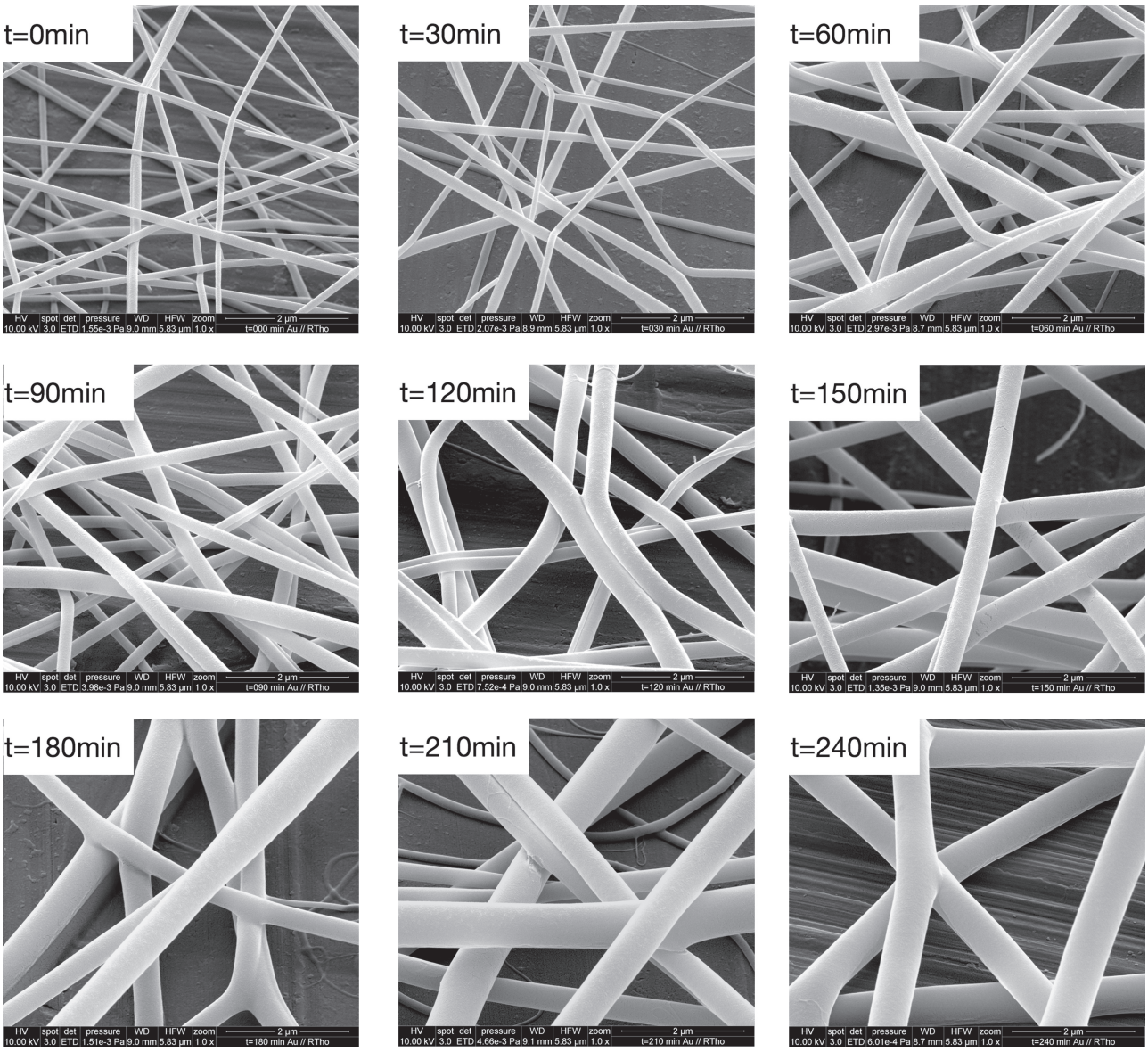

Figure 4. SEM images of glyoxal-mediated in situ crosslinking of gelatin nonwovens (gel14/158 in Table 1): Influence of the electrospinning duration and viscosity built-up on the average fiber size and gradient formation.

crosslinking. **Figure 5** shows the decrease in the primary amine content of gelatin with increasing glyoxal/gelatin (mole/weight) ratio. The higher the glyoxal content in the spin dope, the lower was the resulting content of primary amine groups. Assuming that imidazolium crosslinks[46] are formed when the primary amine group of the lysine moiety reacts with glyoxal, at least one mole of glyoxal should react with one mole of primary amine group. This means that complete crosslinking of the gelatin powder requires at least $(30.5 \pm 0.7) \times 10^{-5}$ mol glyoxal per gram gelatin (cf. Table 3). In all our experiments we used a glyoxal excess of at least 1.37 equivalents. The highest glyoxal excess of 6.3 equivalents gave the highest observed primary amine conversion of 76.4%.

2.3. Cell Tests

To investigate whether the CGN enables cell adhesion and growth, periodontal tissue cells, i.e. human gingival keratinocytes

Table 2. Fiber gradient formation during electrospinning.

Time [min]	0	30	60	90	120	150	180	210	240
Fiber diameter [nm]	90 ± 40	140 ± 60	180 ± 80	230 ± 70	370 ± 110	380 ± 90	540 ± 170	570 ± 180	680 ± 80

Table 3. Water uptake, primary amine content, and amine conversion of CGN nonwovens.

Sample	Content of primary amines [10^{-5} mol·g^{-1}]	Conversion of primary amines [%]	Water uptake [%]
gel14/42	15.0 ± 0.4	50.8	370 ± 30
gel14/74	10.3 ± 0.6	66.2	260 ± 13
gel14/158	8.3 ± 0.4	72.8	270 ± 11
gel14/195	7.2 ± 0.3	76.4	280 ± 10
gelatin powder	30.5 ± 0.7	0	soluble

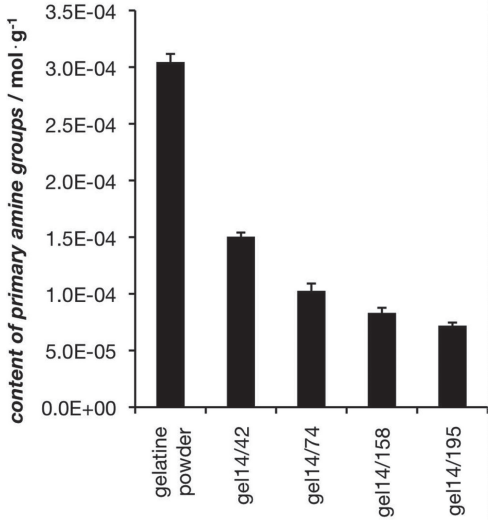

Figure 5. TNBS assay: Measuring the influence of the glyoxal/gelatin ratio (mol·g^{-1}) on the residual content of primary amines after electrospinning.

(GKs) and human gingival fibroblasts (GFs), were seeded on the membrane. **Figure 6**a shows the GKs after a cultivation period of 48 h. The GKs adhered very well to the CGN and exhibited their typical cell morphology. Figure 6b shows that the GFs formed an almost confluent layer on the CGN. To substantiate these findings we investigated single cells on thin layers of CGN using fluorescent microscopy. Staining for F-actin revealed that the GKs were bridged between the fibers (Figure 6c, green) and that the GFs adhered to the fibers. The F-actin fiber network bridged the gelatin meshwork (Figure 6c). Indirect immunofluorescence of vinculin, a focal contact associated protein, (Figure 6c,d, red) revealed co-localization with F-actin, particularly where the cells were adhering to the CGN fibers (Figure 6c,d, arrows).

2.4. Laminated CGN/PCL Hybrid Systems

In spite of the remarkable stability of CGN nonwovens in aqueous media, it is important to further improve their mechanical stability because they are relatively weak and cannot be attached to tissue by means of surgical sutures. To improve mechanical stiffness without sacrificing the benefits of collagenous nanofiber nonwovens, we laminated two CGN layers with one layer of micrometer-sized PCL fiber nonwovens, produced by means of 3D microextrusion of PCL melts, thus producing CGN/PCL/CGN sandwich structures. The lamination process to produce modular scaffold systems is illustrated in **Figure 7**. The average mesh size of the PCL nonwovens was 1 mm with a strand diameter of 0.4 mm. The CGN/PCL/CGN layered system was bonded together by compression molding for 2 h at 80 °C, which is well above the PCL melting temperature. Most likely, this annealing may also contribute to driving gelatin crosslinking to higher degrees of conversion. In this facile lamination process, the perforated PCL layer simultaneously serves as a hotmelt adhesive patch and as reinforcement for the CGN matrix. Bonding at ambient temperature by means of bioadhesives is also possible to enable the use of temperature-sensitive components. In this modular approach there is no need to implement electrospinning directly into the 3D microextrusion process. In general, different types of CGN nonwovens as well as many other layers and materials can be combined at will to produce comparatively complex multilayered biocomposites and novel gradient materials. For instance, instead of using 3D-plotted nonwovens, alternatives for this lamination process include electrospun polyester nonwovens, polyester fabrics with larger mesh sizes, perforated polyester films, conventional hotmelt patches, hot melt dispensing of adhesives, and other adhesive technologies.

The mechanical properties were examined by immersing the CGN nonwovens and the laminated CGN/PCL/CGN sandwich scaffold in distilled water for one hour prior to stress/strain testing. The mechanical properties are listed in **Table 4**. Upon laminating two layers of CGN with one layer of PCL nonwoven, the Young's modulus of the CGN/PCL/CGN scaffold (3.9 ± 1.4 MPa) was almost five times higher than that of CGN (0.88 ± 0.16 MPa). Varying the layers and their stacking sequences offers unique opportunities for designing gradients and tailoring mechanical properties, biodegradation rates, and even biological functions.

3. Conclusion

In conclusion, adding glyoxal as the crosslinking agent to a fluorine-free solution of gelatin in a mixture of acetic acid, water, and ethyl acetate (5:1:2 w/w/w) represents a very facile and versatile one-step process, enabling scale-up and fabrication of collagenous nonwovens based on in situ crosslinked gelatin nanofibers (CGN). This in situ crosslinking renders water-soluble gelatin fibers water-resistant without adversely affecting hydrophilicity, excellent fiber wetting, cell compatibility, resorption, cell adhesion, and cell adhesion and proliferation typical of crosslinked collagenous nanofiber nonwovens. It is possible to control the viscosity increase during the electrospinning process by increasing the glyoxal content, thus enabling in-process formation of gradient CGN nonwovens with fiber diameters gradually varying from 90 to 680 nm. This versatile process and the tailored CGN gradient nonwovens play a key role in mimicking ECM formation in scaffold fabrication. In spite of their good water resistance, the mechanical properties and robustness of CGN nonwovens are greatly improved when they are laminated with bioresorbable nonwovens of micrometer-sized thermoplastic (bio)polymers. This new concept has been demonstrated for layered CGN/PCL

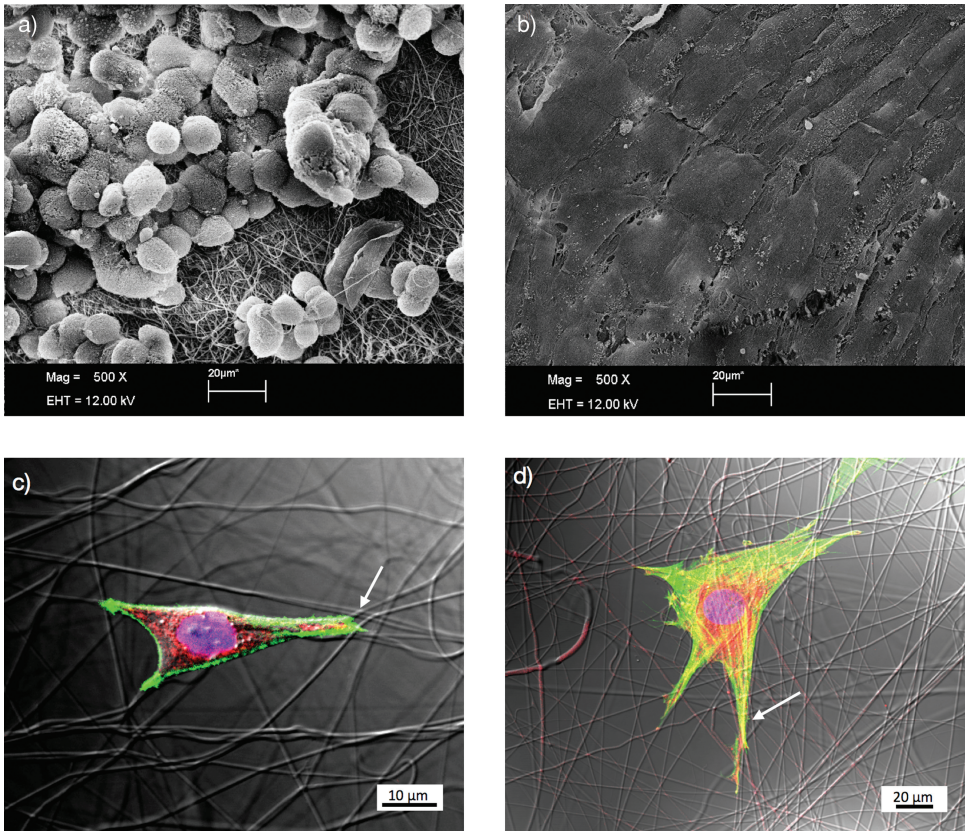

Figure 6. SEM images of a) GKs and b) GFs seeded on the CGN. Fluorescence microscope images of c) stained GKs and d) GFs on thin layers of CGN.

biocomposites using PCL nonwovens, produced by 3D microextrusion of PCL melts, as a hotmelt adhesive patch and fiber reinforcement of CGN. Compression molding and heating of the CGN/PCL multilayer assemblies above the melting temperature of the PCL produces mechanically robust CGN/PCL systems, thus providing new opportunities for the envisioned application in surgery and tissue regeneration. Whereas CGN nonwovens are comparatively weak, the CGN/PCL hybrid scaffolds are robust and can be attached to healthy tissue by means of surgical sutures. Such laminates can be cut into any shape, thus meeting the individual needs of patients requiring tissue engineering. Going well beyond the scope of melt lamination, the CGNs can be laminated and bonded together using a large variety of bioresorbable polymer fabrics, nonwovens, patches, films, and other bioadhesives. The integration of electrospinning into polyester microextrusion is not required. Facile variation of types, composition, numbers, stacking mode, and properties of layers in laminated CGN gradient nonwovens offers unique opportunities for combining the excellent biological properties, such as ECM formation, cell adhesion, and cell proliferation that are typical of CGN nonwovens, with gradient formation and fiber reinforcement that are required in surgical applications.

4. Experimental Section

Electrospinning of Gelatin Solutions: Gelatin solutions were prepared by dissolving gelatin powder (Merck, EMPROVE) in a solvent mixture of acetic acid (Sigma Aldrich Germany, puriss. p.a.), ethyl acetate (Merck, EMSURE) and water (5:3:2 w/w/w), similar to the procedures reported by Song et al..[25,27] After stirring for four hours, a clear solution (14 wt%) was obtained. Prior to electrospinning, the solution was mixed with the desired amount of glyoxal solution (Sigma Aldrich Germany, BioReagent 40% in H_2O). The resulting mixture was transferred into a syringe and dispensed by means of a syringe pump (KDS 100, KD scientific) with a flow rate of 0.5 mL/h. The spinneret was a capped hypodermic needle with a diameter of 0.8 mm (Gauge 21) from Braun. The tip was connected to a high-voltage power supply (Heinzinger LNC 30000), which generates an electric field (0.4 to 8 kV/cm) between the tip of the syringe nozzle and the collector (alumina foil). Subsequently, the fiber mats were placed in an oven (80 °C) for two hours to obtain the CGN. For fluorescent microscopy, only small amounts of gelatin solution (0.1–0.2 mL) were spun on cover slips.

3D Microextrusion of PCL: PCL (Durect, Cupertino, USA) with a M_W of 98 000 g/mol and an intrinsic viscosity of 1.29 dl/g was filled into the heated cartridge of the printhead using the 3D-Bioplotter (third generation, Envisiontec, Gladbeck, Germany); with a printhead driving speed v(xy) of 560 mm/min, temperature 190 °C, pressure 0.96 bar, nozzle diameter 0.8 mm. All structures were printed onto standard printer paper (80 gm^{-2}, m-real, Metsä, Finland).

Rheology: For the rheological measurements and monitoring of the gelatin crosslinking, a stress-controlled rheometer (Paar Physica UDS200) with a parallel-plate geometry was used. The solution was placed between the plates. To avoid solvent evaporation, the gap was covered with an immiscible silicone oil (Wacker silicone fluid AK 150). For the time-sweep experiments we choose a 50 mm plate with gap $H_0 = 0.67$ mm. The deformation γ_0 was 30%, the circular frequency ω was 1 rad/s, and the temperature T was 25 °C.

Fiber and Nonwoven Morphologies: The electrospun nonwovens were sputtered with gold for three minutes and investigated with a Quanta

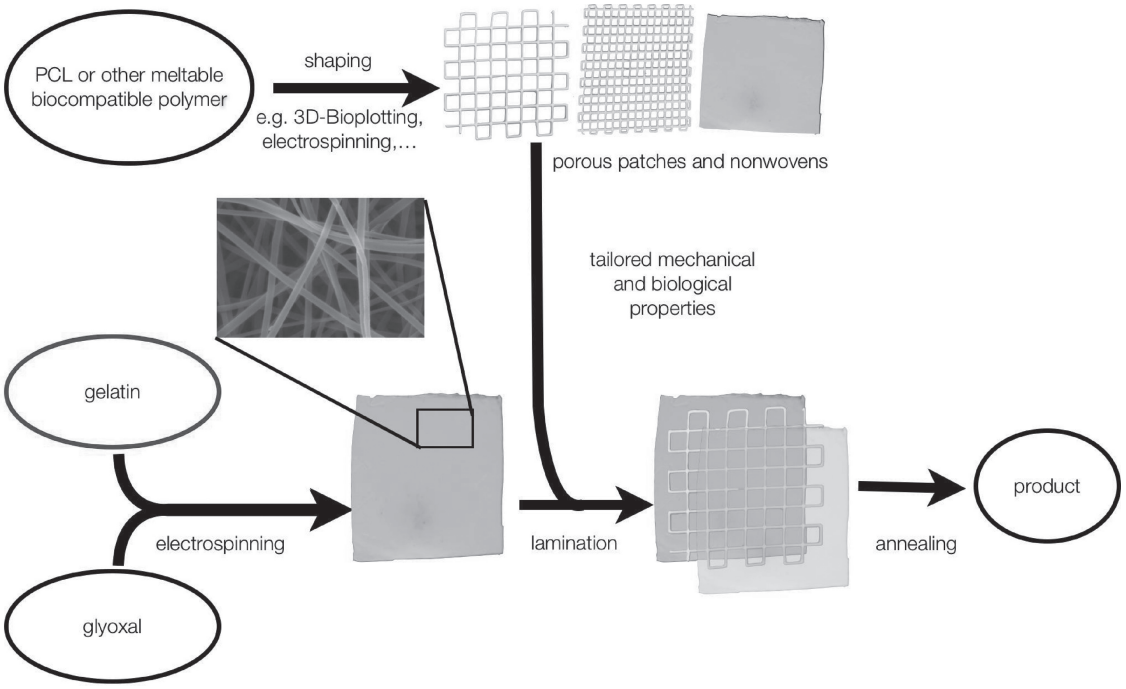

Figure 7. Scheme for the production of CGN/PCL biocomposite scaffolds.

Table 4. Tensile testing of CGN/PCL micro-/nanohybrid scaffolds.

Sample ($n = 5$)	Young's modulus [MPa]	Elongation at break [%]	Maximum strength [MPa]
CGN nonwoven	0.88 ± 0.16	180 ± 40	3.2 ± 0.5
CGN/PCL laminate	3.9 ± 1.4	45 ± 3	1.48 ± 0.17

FEG 250 (FEI, Eindhoven, The Netherlands) at an accelerating voltage of 10 kV. The fiber diameter was measured using the image analysis software Image J (National Institutes of Health, USA). The average diameter and the standard deviation were calculated from one hundred random measurements of each sample.

SEM Observation of Cell-Loaded CGN: The membrane was cut into circular pieces with a diameter of 15 mm that were placed in 24-well plates (Becton Dickinson, Heidelberg, Germany). The membranes were sterilized and equilibrated in PBS as described above. Then 5×10^4 cells/cm^2 GF and 1×10^5 cells/cm^2 GK were seeded separately in their respective cultivation medium. After a cultivation period of 48 h, the test specimens were fixed with 3.8% formaldehyde in PBS for at least 1 h and rinsed three times with PBS. The specimens were then dehydrated by rinsing them through graded ethanol/water mixtures (50%, 70%, 80%, 90%, and 100%; 10 min at RT for each step). Ethanol was then slowly exchanged by liquid CO_2 (critical point dryer; Balzers CPD, Balters Union). Finally, the samples were dried using the critical-point method,[47] sputtered with a thin layer of gold of approximately 10 nm in thickness (sputter coater, Balzers SLD; Balzers Union), and examined under a Leo 435VP (Zeiss) scanning electron microscope.

TNBS Assay: For TNBS assays we used a procedure reported by Bubnis and Ofner.[44] Between 6–12 mg of collagenous material was placed in a vial. $NaHCO_3$ solution (4 wt%; 1 mL) and TNBS solution (0.5%; 1 mL) were added. The mixture was shaken at 40 °C and 250 min^{-1} for 4 h. HCl (6 M; 3 mL) was added, and the mixture was shaken at 50 °C until all of the collagenous material had dissolved. The blanks for each sample were prepared by the same procedure as the samples but the HCl was added before the TNBS solution. The hydrolyzed samples were diluted with H_2O (5 mL) and extracted with Et_2O (3×5 mL). An aliquot (5 mL) of the aqueous phase was removed, and nitrogen was bubbled through for 5 min to remove residual ether. The aliquot was diluted with distilled water (15 mL), and the absorbance at 346 nm was measured with a Perkin-Elmer Lambda 2 UV-vis spectrometer.

Swelling Test: The collagenous material (25–50 mg) was left to swell in distilled water at 37 °C. The samples were shaken at 250 min^{-1} for 24 h and then pressed between filter paper until no further wetting of the paper was visible. The degree of swelling q was calculated with the following equation: $q = (m_s\text{-}m_i)\cdot m_i^{-1}\cdot 100\%$, where m_i and m_s are the sample weights before and after swelling, respectively.

Mechanical Characterization: The tensile tests were performed on a Zwick Z005. The scaffolds were cut into rectangular pieces measuring 5 mm × 40 mm with a thickness between (0.015 to 0.03) mm. These pieces were soaked with distilled water before testing. We used a 100 N load cell and a strain rate of 1 mm/min.

Cell Culture: Cultures of primary gingival fibroblasts (GFs) were established by the explants technique.[48] Tissue harvesting from patients was performed according to the Helsinki Declaration, and approved by the institutional ethics committee. For routine cell cultures, the cells were maintained in Dulbecco's Modified Eagle's Medium (DMEM, PAA, Cölbe, Germany) containing 10% fetal calf serum (FCS, Biochrom AG, Berlin, Germany) and 50 mg/mL kanamycin (Sigma-Aldrich, Munich, Germany). Passages 8–12 were used for the in-vitro experiments. To exclude alterations of cell morphology induced by cell senescence and the expression of tissue-specific biomarkers, the periodontal cells were previously tested for consistent expression of the respective biomarkers and their native cell morphology over time. Human gingival keratinocytes (GKs) have been established as an immortalized cell line and their characterization and serial cultivation was recently reviewed.[49] During routine cell culture, the GKs were maintained in a keratinocyte growth medium (KGM2, PromoCell, Heidelberg, Germany) that contained the necessary supplements and 50 mg/mL kanamycin (Sigma-Aldrich, Munich, Germany).

Fluorescent Microscopy of GFs and GKs on CGN: The cytoskeleton and cell adhesion-related biomarkers were investigated by fluorescent microscopy using the above-described cover slips coated with gelatin

fibers. The coated cover slips were first sterilized with 70% ethanol for 15 min, rinsed thoroughly with phosphate-buffered saline (PBS, Invitrogen, Karlsruhe, Germany) and equilibrated overnight in PBS. For single-cell observations, 1×10^4 cells/cm^2 GF and 3×10^4 cells/cm^2 GK were seeded separately on gelatin fiber-coated cover slips and cultured in their respective culture medium. The cells were maintained under standard cell-culture conditions at 37 °C, 97% humidity, and 5% CO_2. After cultivation for 24 h, the cells were fixed with 3.8% formaldehyde in PBS for 15 min and rinsed with PBS three times. The cells were then permeabilized with 0.2% Triton-X-100 (Roche, Mannheim, Germany) for 5 min and washed again with PBS three times. To block unspecific binding sites, the specimens were incubated with Image-iT-FX enhancer (Invitrogen, Karlsruhe, Germany) for 30 min and rinsed thoroughly with PBS. Subsequently, the actin cytoskeleton was stained by incubating the specimens with Phalloidin-Alexa 488 (wd = 1:40, Invitrogen, Karlsruhe, Germany) for 45 min at RT, followed by washing with PBS three times for 5 min each. The cell adhesion-related biomarkers were detected by incubating with a vinculin-specific primary antibody (wd = 1:50, Abcam, Cambridge, UK) for 1 h at RT. After washing the specimens with PBS three times for 5 min each, samples were incubated with an Alexa 594-labelled secondary antibody (wd = 1:200, Invitrogen, Karlsruhe, Germany) for 45 min, followed by three washing steps with PBS for 5 min each. Nuclear counterstaining was performed with a 300 nM DAPI solution (Invitrogen, Karlsruhe, Germany) in PBS for 10 min, and the cells were subsequently washed three times with PBS followed by rinsing once with distilled water. Finally, the specimens were embedded in Fluoromount-G (SouthernBiotech, Birmingham, AL, USA) and examined by laser scanning fluorescent microscopy (Leica TCS SP2 AOBS; Leica, Wetzlar, Germany).

Acknowledgements

The authors are grateful to the Ministry of Science, Research and Art of the German State of Baden-Württemberg for supporting this research on bioinspired adhesive patches (720.830-5-4a, "Molekulare Bionik").

Received: September 27, 2012
Revised: December 12, 2012
Published online: February 6, 2013

[1] Y. Xia, *Nat Mater* **2008**, *7*, 758–760.
[2] R. Langer, D. A. Tirrell, *Nature* **2004**, *428*, 487–492.
[3] P. X. Ma, *Adv. Drug Delivery Rev.* **2008**, *60*, 184–198.
[4] J. Lannutti, D. Reneker, T. Ma, D. Tomasko, D. Farson, *Mater. Sci. Eng., C* **2007**, *27*, 504–509.
[5] J. Xie, X. Li, Y. Xia, *Macromol. Rapid Commun.* **2008**, *29*, 1775–1792.
[6] A. Greiner, J. H. Wendorff, *Angew. Chem. Int. Ed.* **2007**, *46*, 5670–5703.
[7] M. Li, M. J. Mondrinos, M. R. Gandhi, F. K. Ko, A. S. Weiss, P. I. Lelkes, *Biomaterials* **2005**, *26*, 5999–6008.
[8] H. Yoshimoto, Y. M. Shin, H. Terai, J. P. Vacanti, *Biomaterials* **2003**, *24*, 2077–2082.
[9] S. Shortkroff, Y. Li, T. S. Thornhill, G. C. Rutledge, *Abstr. Pap. Am. Chem. Soc.* **2002**, *224*, U504.
[10] W. J. Li, R. Tuli, X. X. Huang, P. Laquerriere, R. S. Tuan, *Biomaterials* **2005**, *26*, 5158–5166.
[11] Q. P. Pham, U. Sharma, A. G. Mikos, *Biomacromolecules* **2006**, *7*, 2796–2805.
[12] F. Yang, R. Murugan, S. Wang, S. Ramakrishna, *Biomaterials* **2005**, *26*, 2603–2610.
[13] A. S. Badami, M. R. Kreke, M. S. Thompson, J. S. Riffle, A. S. Goldstein, *Biomaterials* **2006**, *27*, 596–606.
[14] X. Zong, H. Bien, C.-Y. Chung, L. Yin, D. Fang, B. S. Hsiao, B. Chu, E. Entcheva, *Biomaterials* **2005**, *26*, 5330–5338.
[15] Y. Zhang, H. Ouyang, C. T. Lim, S. Ramakrishna, Z.-M. Huang, *J. Biomed. Mater. Res.* **2005**, *72B*, 156–165.
[16] V. Y. Chakrapani, A. Gnanamani, V. R. Giridev, M. Madhusoothanan, G. Sekaran, *J. Appl. Polym. Sci.* **2012**, *125*, 3221–3227.
[17] H.-W. Kim, H.-S. Yu, H.-H. Lee, *J. Biomed. Mater. Res.* **2008**, *87A*, 25–32.
[18] J. J. Han, P. Lazarovici, C. Pomerantz, X. S. Chen, Y. Wei, P. I. Lelkes, *Biomacromolecules* **2011**, *12*, 399–408.
[19] W. Cui, X. Li, J. Chen, S. Zhou, J. Weng, *Cryst. Growth Des.* **2008**, *8*, 4576–4582.
[20] Z. W. Ma, W. He, T. Yong, S. Ramakrishna, *Tissue Eng.* **2005**, *11*, 1149–1158.
[21] S. Agarwal, J. H. Wendorff, A. Greiner, *Adv. Mater.* **2009**, *21*, 3343–3351.
[22] S. Panzavolta, M. Gioffrè, M. L. Focarete, C. Gualandi, L. Foroni, A. Bigi, *Acta Biomater.* **2011**, *7*, 1702–1709.
[23] J. D. Schiffman, C. L. Schauer, *Biomacromolecules* **2007**, *8*, 2665–2667.
[24] Y. Z. Zhang, J. Venugopal, Z.-M. Huang, C. T. Lim, S. Ramakrishna, *Polymer* **2006**, *47*, 2911–2917.
[25] K. Sisson, C. Zhang, M. C. Farach-Carson, D. B. Chase, J. F. Rabolt, *Biomacromolecules* **2009**, *10*, 1675–1680.
[26] T. Nguyen, B. Lee, *J. Biomed. Sci. Eng.* **2010**, *3*, 1117–1124.
[27] J.-H. Song, H.-E. Kim, H.-W. Kim, *J. Mater. Sci.* **2008**, *19*, 95–102.
[28] L. Meng, O. Arnoult, M. Smith, G. E. Wnek, *J. Mater. Chem.* **2012**, *22*, 19412–19417.
[29] K. F. Leong, C. M. Cheah, C. K. Chua, *Biomaterials* **2003**, *24*, 2363–2378.
[30] D. W. Hutmacher, S. Cool, *J. Cell. Mol. Med.* **2007**, *11*, 654–669.
[31] N. Sudarmadji, J. Y. Tan, K. F. Leong, C. K. Chua, Y. T. Loh, *Acta Biomater.* **2011**, *7*, 530–537.
[32] K. F. Leong, C. K. Chua, N. Sudarmadji, W. Y. Yeong, *J. Mech. Behav. Biomed. Mater.* **2008**, *1*, 140–152.
[33] P. J. Bártolo, C. K. Chua, H. A. Almeida, S. M. Chou, A. S. C. Lim, *Virtual Phys. Prototyping* **2009**, *4*, 203–216.
[34] C. K. Chua, K. F. Leong, N. Sudarmadji, M. J. J. Liu, S. M. Chou, *MRS Bull.* **2011**, *36*, 1006–1014.
[35] E. Sachlos, J. T. Czernuszka, *Eur. Cells Mater.* **2003**, *5*, 29–40.
[36] M. Gurr, R. Mülhaupt *Rapid Prototyping*, Elsevier: Amsterdam, **2012**, pp. 77–99.
[37] A. Pfister, R. Landers, A. Laib, U. Hübner, R. Schmelzeisen, R. Mülhaupt, *J. Polym. Sci. A Polym. Chem.* **2004**, *42*, 624–638.
[38] G. Kim, J. Son, *Appl. Phys. A: Mater. Sci. Process.* **2009**, *94*, 781–785.
[39] K. Haberstroh, K. Ritter, J. Kuschnierz, K.-H. Bormann, C. Kaps, C. Carvalho, R. Mülhaupt, M. Sittinger, N.-C. Gellrich, *J. Biomed. Mater. Res.* **2010**, *93B*, 520–530.
[40] A. Al-Ahmad, M. Wiedmann-Al-Ahmad, C. Carvalho, M. Lang, M. Follo, G. Braun, A. Wittmer, R. Mülhaupt, E. Hellwig, *J. Biomed. Mater. Res.* **2008**, *87A*, 933–943.
[41] L. Moroni, R. Schotel, D. Hamann, J. R. de Wijn, C. A. van Blitterswijk, *Adv. Funct. Mater.* **2008**, *18*, 53–60.
[42] H. Yoon, S. Ahn, G. Kim, *Macromol. Rapid Commun.* **2009**, *30*, 1632–1637.
[43] M. G. Yeo, G. H. Kim, *Chem. Mater.* **2011**, *24*, 903–913.
[44] W. A. Bubnis, C. M. Ofner, *Anal. Biochem.* **1992**, *207*, 129–133.
[45] I. I. I. Ofner, M. Clyde, W. A. Bubnis, *Pharm. Res.* **1996**, *13*, 1821–1827.
[46] K. J. Wells-Knecht, E. Brinkmann, J. W. Baynes, *J. Org. Chem.* **1995**, *60*, 6246–6247.
[47] W.-Y. Yeong, C.-K. Chua, K.-F. Leong, M. Chandrasekaran, M.-W. Lee, *J. Biomed. Mater. Res.* **2007**, *82B*, 260–266.
[48] P. Tomakidi, D. Breitkreutz, N. E. Fusenig, J. Zöller, A. Kohl, G. Komposch, *Cell Tissue Res.* **1998**, *292*, 355–366.
[49] M. Roesch-Ely, T. Steinberg, B. Xavier, F.E. Müssig, N. Whitaker, T. Wiest, A. Kohl, G. Komposch, P. Tomakidi, *Differentiation* **2006**, *74*, 622–637.